Published in final edited form as:
Curr Alzheimer Res. 2011 May 1; 8(3): 313–322.

Changes in the Expression of the Alzheimer's Disease-Associated Presenilin Gene in *Drosophila* Heart Leads to Cardiac Dysfunction

A. Li[1], **C. Zhou**[2], **J. Moore**[1], **P. Zhang**[3], **T.-H. Tsai**[2], **H.-C. Lee**[2], **D.M. Romano**[1], **M.L. McKee**[4], **D.A. Schoenfeld**[5], **M.J. Serra**[3], **K. Raygor**[1], **H.F. Cantiello**[3], **J.G. Fujimoto**[2,*], and **R.E. Tanzi**[1,*]

[1] Genetics and Aging Research Unit, Department of Neurology, MassGeneral Institute for Neurodegenerative Diseases, Massachusetts General Hospital and Harvard Medical School, MA, USA

[2] Department of Electrical Engineering and Computer Science, Massachusetts Institute of Technology, MA USA

[3] Department of Medicine, Massachusetts General Hospital and Harvard Medical School, MA; USA

[4] Program in Membrane Biology, Massachusetts General Hospital and Harvard Medical School, MA, USA

[5] Department of Biostatistics, Harvard School of Public Health, MA, USA

Abstract

Mutations in the presenilin genes cause the majority of early-onset familial Alzheimer's disease. Recently, presenilin mutations have been identified in patients with dilated cardiomyopathy (DCM), a common cause of heart failure and the most prevalent diagnosis in cardiac transplantation patients. However, the molecular mechanisms, by which presenilin mutations lead to either AD or DCM, are not yet understood. We have employed transgenic *Drosophila* models and optical coherence tomography imaging technology to analyze cardiac function in live adult *Drosophila*. Silencing of *Drosophila* ortholog of presenilins (*dPsn*) led to significantly reduced heart rate and remarkably age-dependent increase in end-diastolic vertical dimensions. In contrast, overexpression of *dPsn* increased heart rate. Either overexpression or silencing of *dPsn* resulted in irregular heartbeat rhythms accompanied by cardiomyofibril defects and mitochondrial impairment. The calcium channel receptor activities in cardiac cells were quantitatively determined via real-time RT-PCR. Silencing of *dPsn* elevated dIP_3R expression, and reduced *dSERCA* expression; overexprerssion of *dPsn* led to reduced *dRyR* expression. Moreover, overexpression of *dPsn* in wing disc resulted in loss of wing phenotype and reduced expression of wingless. Our data provide novel evidence that changes in presenilin level leads to cardiac dysfunction, owing to aberrant calcium channel receptor activities and disrupted Wnt signaling transduction, indicating a pathogenic role for presenilin mutations in DCM pathogenesis.

[*]Address correspondence to these authors at the Genetics and Aging Research Unit, Department of Neurology, Massachusetts General Hospital, 114, 16th Street, Charlestown, MA 02129, USA; Tel: 617 726 6845; Fax: 617 724 1949; tanzi@helix.mgh.harvard.edu; and Department of Electrical Engineering and Computer Science, Massachusetts Institute of Technology, 77 Massachusetts Avenue, Cambridge, MA 02139, USA; Tel: 617 253 8528; Fax: 617 253 9611; jgfuji@mit.edu.

Keywords

Alzheimer's disease; calcium channel; cardiomyopathy; Drosophila; heart; presenilin

INTRODUCTION

Alzheimer disease (AD) is a progressive neurodegenerative disorder and the most common form of dementia in the elderly, affecting one in 10 individuals over 65 and nearly half over 85 years old (http://www.alz.org/). The presenilin 1 and 2 genes (*PSEN1* and *PSEN2*) encode highly conserved polytopic membrane proteins (PS1 and PS2) that are required for γ-secretase activity [1]. Mutations in presenilins underlie the majority of cases of early-onset familial AD. Most mutations in presenilins increase the relative ratio between the longer (Aβ42) and shorter (Aβ40) amyloid peptides (Aβ42/Aβ40) [2]. Aβ42 is the main component of amyloid plaques in the brains of AD patients, and the progressive formation of amyloid plaques is regarded as a key neuropathological feature of AD [3]. Recently, mutations in presenilins have also been reported in dilated cardiomyopathy (DCM) patients [4, 5], indicative of allelic heterogeneity. DCM is defined clinically by dilation and impaired contraction of one or both ventricles. DCM occurs in all ages, most common between 20–60 years. DCM causes roughly one-third of cases of congestive heart failure and is the most prevalent diagnosis in individuals referred for cardiac transplantation. Half of DCM patients die within 15 years after diagnosis [6]. Presenilin mutations were identified in DCM patients in the *PSEN1* 5′ promoter and a large cytoplasmic loop between transmembrane domains six and seven, and *PSEN2* NH_2 terminus [4, 5]. Presenilin mutations have also commonly been found in 20% of severe DCM patients who required heart transplantation due to heart failure [5]. The *PSEN1* 5′ promoter region variants in DCM patients led to significant reduction in transcriptional activities and decreased expression of PS1 protein in the myocardium [5]. The *PSEN2-R62H* missense mutation in DCM patients enhanced PS2 degradation, reduced PS2 stability in mouse embryonic fibroblasts, and altered compromised PS2 function in Notch signaling in C. elegans [7]. Together, these data suggest that *PSEN1* and *PSEN2* mutations or variants contribute to DCM pathogenesis through loss of gene function, and implicate novel mechanisms of cardiomyopathy.

Both AD and DCM are associated with high morbidity and mortality, but currently have no cure. The molecular mechanisms by which presenilin mutations lead to DCM pathogenesis are not yet understood. AD brain contains Aβ oligomers, which have been shown to impair neurotransmission [8]. Likewise, amyloid oligomers have been found in the failing heart of DCM patients associated with cardiomyocyte apoptosis [5], in cardiomyocytes derived from human heart-failure patients, and in mice model of desmin-related cardiomyopathy [9]. Protein misfolding is implicated in the etiology and pathogenesis of both AD and DCM [5]. Apolipoprotein E (APOE) is a multifunctional protein that plays a key role in the metabolism of cholesterol and triglycerides; *APOE* gene *ε4* variant is not only the largest known genetic risk factor for late-onset AD [10], but also increases both low-density lipoprotein cholesterol level and coronary heart disease risk [11]. Moreover, cerebral angiopathy contributes to cognitive decline and dementia in AD patients and mouse models [12]. The expression of vascular *MEOX2* is low in AD; silencing of *MEOX2* in brain capillaries results in aberrant brain angiogenesis, reduced vascular density and faulty clearance of Aβ [13]. These indicate the connection between AD and cardiovascular diseases.

PSEN1 and *PSEN2* are strongly expressed in the heart and essential for cardiac morphogenesis [14, 15]. To date, there is no reported information regarding the *in vivo* functional role of PS1 in adult heart. Mice null for Ps1 are either dead at birth ($Ps1^{-/-}$) or

embryonically lethal ($Ps1^{-/-}/Ps2^{-/+}$), exhibiting multiple developmental defects including a cardiac anomaly [15]. The basic mechanisms of heart development and control of cardiac function are highly conserved between human and *Drosophila melanogaster*, or the fruit fly, which has been successfully used to characterize genes associated with human diseases, including cardiomyopathy [16, 17]. Moreover, the morphological and rhythm changes can be readily analyzed in the relatively simple organization of fly heart with an emerging medical imaging technology optical coherence tomography (OCT) [16, 18, 19]. OCT enables real-time, *in vivo*, micron-scale and three-dimensional imaging of biological tissues [20]. OCT has been used for a wide range of clinical applications in human, including ophthalmology, endoscopy, cardiovascular imaging [20–22], and recently, studying cardiac functions in live *Drosophila* [23].

The human *PSEN1* and *PSEN2* are represented by a highly conserved single ortholog, *dPsn*, in *Drosophila* [24, 25]. To better understand the pathogenic role(s) of presenilin mutations in DCM, we have employed transgenic *Drosophila* models to analyze the effects of overexpression or RNAi silencing of *dPsn* on cardiac function, assessed by employing the noninvasive OCT technology. In addition, we also examined heart ultrastructure, calcium channel receptor level, wing development and expression of the wingless (wg) protein, the central component of Wnt signaling transduction pathway that regulates cardiac development.

MATERIAL AND METHODS

Transgenic Flies and Fly Culture

Fly culture and crosses were carried out according to standard procedures. The following fly strains were used: *GMR-GAL*4 [26, 27], *Sd-GAL4* [28], *Ptc-GAL4* [29], *24B-GAL4* [30], 2XUAS-dPsn; GMR-GAL4 [25] and UAS-$dPsn^{RNAi}$ [31].

Optical Coherence Tomography (OCT) for Drosophila Cardiac Function Assessment

The OCT system used is modified based on a swept source OCT engine (Thorlabs Inc).

To study the cardiac function, the flies were anesthetized with Fly Nap for 2 minutes and mounted on glass slides before imaging. Two-dimensional cross-sectional images consisting 64 A-lines covering 250 μm over the heart chamber were continuously acquired for 5 seconds at ~120 fps. The imaging plane was consistently chosen to be within segments A6–A7 of the *Drosophila* heart chamber. This OCT system achieved a finer imaging resolution and significantly improved imaging speed compared to previously reported OCT apparatus for *Drosophila* heart imaging [23]. Three to four repeated measurements were acquired for each fly. The same experimental groups were repeatedly measured and the results were included in the final data. Post-processing the image data was performed with custom written Matlab (Math-works, Inc) codes to obtain the dimensions of the heart chamber for each frame. M-mode image over the center of the chamber was generated together with the dimension over time. Functional parameters, including heart rate (HR, beat per minute, BPM), rhythmicity of the heartbeat, and the end-systolic and end-diastolic vertical dimensions (ESD and EDD, μm) and fraction shorting (FS, %), were extracted from the dimension plots. The prevalence of arrhythmia was quantitatively analyzed via identifying irregular heartbeat rhythm in the dimension plots for the number of arrhythmia flies in each group (%).

Heart Ultrastructure Analysis by Transmission Electron Microscopy

10–15 fly hearts from 30-day-old flies of each genotype group were fixed, embedded, sectioned and examined as modified from previously in a JEOL JEM 1011 transmission

electron microscope for ultrastructure analyses [32]. In brief, tissues were fixed in glutaraldehyde, stained en bloc, dehydrated through a graded series of ethanol and then embedded in Epon. Thin sections were cut, collected on formvar-coated grids, stained with uranyl acetate and lead citrate and examined in a JEOL JEM 1011 transmission electron microscope at 80 KV. Images were collected using an Advanced Microscopy Techniques digital imaging system.

Immuno-Staining and Western Blot Analyses

The third instar wing discs were fixed, blocked and probed with primary and secondary anti-bodies accordingly. Wings from adult flies were dissected in isopropanol and mounted in Canada Balsam mounting medium. Western Blot analyses were performed and repeated at least twice using protein isolated from 7-day old fly heart and muscle and the intensity of signals was analyzed using image program Quantity One version 4.6.2. In brief, the levels of analyzed proteins were normalized using the levels of dActin for loading differences controls, and quantification in total protein amounts and presented as the percentage of those in the transgenic flies in comparison with that in controls. The following anti-bodies were used: Mouse anti-wg antibody (Developmental Studies Hybridoma Bank, 1:1000); the secondary anti-mouse Alexa 546 (Invitrogen, 1:200); Rabbit-anti-dPsn (Genescript, against CTF, 1:1000); mouse anti-actin (DSHB; 1:1000).

CDNA synthesis and Real-Time RT-PCR

The cDNAs used for real time RT-PCR were synthesized from total RNA isolated from heart and muscle of 7-day old adult *Drosophila*. The cDNA was synthesized using SUPERSCRIPT Preamplification System for First-Strand cDNA Synthesis (Invitrogen). Real-time RT-PCR quantification with *dIP3R*, *dRyR*, *dSERCA* or *dActin*-specific sense and antisense primers was done on an iCycler (BIORAD) using SYBR Green PCR Core Reagents (Qiagen) according to the manufacturer's instructions. House-keeping gene *dActin* as internal control was co-amplified under the same PCR conditions. All standards and unknown samples were run in triplicates per reaction. The fluorescence intensity was calculated using iCycler software version 3.1. The expressions of dIP_3R, *dRyR* and *dSERCA* were given as relative number of copies (%) of mRNA molecules, as calibrated by co-amplification of *dActin*. dIP_3R, *dRyR* and *dSERCA* levels were shown as Mean ± Standard Deviation (Std) of repeated experiments. *p* values were calculated by two-tailed Student's *t* test. $p<0.05$ is defined statistically significant.

Statistical Analyses of Cardiac Function

The cardiac functions, including HR, ESD and EDD and FS, were compared between 7-day old and 30-day old flies overexpressing or silencing *dPsn* vs. age-matched controls and between 7-day old and 30-day old flies of each genotype group. We used a SAS GLM program for statistical analyses. Results were shown as Mean ± Standard Error (SE). $p<0.05$ is defined statistically significant (actual *p* values are shown).

RESULTS

Cardiac Function and Heart Ultrastructure Analysis

We employed the well established UAS-dPsn or UAS-dPsn-RNAi transgenic flies and *24B-GAL4* driver [30] to overexpress or RNAi silence full-length wild-type (WT) *dPsn* specifically in fly heart and muscle [24, 25, 30, 31]. The *24B-GAL4* line allows targeted expression in mesoderm and all cardiac and muscular cells with a uniform and high level of expression in the most anterior heart cells [33]. Flies in which *dPsn* was either overexpressed or silenced by *24B-GAL4* appeared normal at eclosion. We quantitatively

measured cardiac function, including heart rate (HR, beat per minute, BPM), rhythmicity of the heartbeat, the end-systolic and end-diastolic vertical dimensions -ESD and EDD (μm), fraction shorting (FS, %), in adult flies with a customized OCT system.

We analyzed 7-day and 30-day old adult male flies overexpressing *dPsn* (UAS-dPsn; 24B-GAL4) or RNAi silencing *dPsn* (UAS-dPsn^{RNAi}; 24B-GAL4) in comparison with that of age-matched male controls (24B-GAL4/+) Fig. (1 & 2) (Table 1). Compared with age-matched controls, at either 7-day, 30-day old age group alone, or 7-day and 30-day old combined age group, overexpression of *dPsn* significantly increased HR; in contrast, silencing of *dPsn* significantly decreased HR. Remarkably, either overexpression or RNAi silencing of *dPsn* in heart resulted in very irregular heartbeats: heartbeat rhythm changed rapidly between fast and slow pace within 1–2 seconds, or *vice versa*. Quantitative analysis of arrhythmia prevalence demonstrated that silencing of *dPsn* significantly increased the number of flies with arrhythmia at 30-day old flies (57%) or combined age group (54%) compared to that in age-matched control flies. Likewise, overexpression of *dPsn* resulted in significant increase in the number of flies with arrhythmia at 30-day old flies (46%) compared to 7-day old flies (19%). Control flies aging from 7-day to 30-day old barely changed arrhythmia prevalence (26% to 27%). Overexpression of *dPsn* decreased ESD at 30-day old flies or combined age group. Flies in which *dPsn* was silenced showed significantly reduced ESD (30-day old flies alone and combined age group) and EDD (7-day old flies and combined age group). Compared with 7-day old flies, 30-day old flies in which *dPsn* was silenced exhibited a significant decrease in HR and a remarkable increase in EDD and FS. 30-day old of flies in which *dPsn* was overexpressed or control flies also showed a trend for age-dependent decrease in HR and significant increase in EDD compared with that in 7-day old flies (Table 1).

Consistent with cardiac function alterations, analysis of heart ultrastructure by transmission electron microscopy revealed normal myofibril structure in control flies Fig. (3A). In contrast, myofibrils of heart from flies overexpressing *dPsn* exhibited irregular structure with vacuoles, a broadening of Z-line, and swollen mitochondria Fig. (3B). RNAi silencing of *dPsn* led to an overall decrease in the density of myofibrils with vacuoles, a breaking Z-line, and severely degenerative mitochondria with impaired structure Fig. (3C).

To assess the effects of RNAi silencing or overexpression of *dPsn* in transgenic flies, we carried out Western blot analysis using protein lysates isolated from the heart and muscle of 7-day old flies Fig. (4). Silencing of *dPsn* led to a 60% decrease in dPsn expression, and overexpression of *dPsn* led to a 180% increase in dPsn expression as compared to controls Fig. (4).

Calcium Channel Receptor Expression

In cardiac muscle, Ca^{2+} influx during depolarization of action potential initiates the sequence of events leading to contraction. Ca^{2+} signaling is primarily modulated by the functional properties of Ca^{2+} release channels. There are two main types of Ca^{2+} release channels, the inositol 1,4,5-trisphosphate receptor (IP_3R) and the ryanodine receptor (RyR) [34].

The removal of cytosolic Ca^{2+} allows for relaxation of muscle fibres. The Ca^{2+}uptake into sarcoplasmic reticulum (SR) store occurs predominately by the cardiac isoform of the SR Ca^{2+}-ATPase pump SERCA2a [34]. We have identified that the human *IP_3R*, *RyR* and *SERCA2a* are represented by highly conserved single orthologs in *Drosophila*, as *dIP_3R* (*Itp-r83A*), *dRyR* (*Rya-r44F*) and *dSERCA* (*Ca-P60A*) (www.flybase.org). We quantitatively determined the expression of *dIP_3R*, *dRyR* and *dSERCA* levels via real-time RT-PCR amplification of cDNA samples from 7-day old flies in which *dPsn* was overexpressed

(UAS-dPsn; 24B-GAL4), or silenced (UAS-dPsn^{RNAi}; 24B-GAL4) and control (24B-GAL4/+). *dIP$_3$R*, *dRyR* and *dSERCA* levels were normalized by co-amplified internal control gene *dActin*. *dIP$_3$R* expression levels were 1.17 fold higher in flies overexpressing *dPsn*, and 2.19-fold higher in flies *dPsn* was silenced as compared to controls Fig. (5A). Overexpressing of *dPsn* led to significantly decreased *dRyR* expression (60% of control levels), while silencing of *dPsn* slightly increased *dRyR* expression (1.05-fold of control levels) Fig. (5B). Furthermore, overexpressing of *dPsn* slightly increased *dSERCA* expression (1.1-fold of control levels), and silencing of *dPsn* significantly decreased *dSERCA* expression (40% of control levels) Fig. (5C).

Wing Development and Wingless Expression

The UAS promoter used in the *dPsn* transgenic models allows for conditional overexpression or silencing of *dPsn* with specific GAL4 drivers in the wing or other tissues, in addition to heart. *Drosophila* adult wing and thoracic body wall arise from the larval wing disc. Wing development is regulated by multiple signaling pathways, including Wnt, Notch, epidermal growth factor receptor, hedgehog and de-capentaplegic. The wing pattern provides an important tool in isolating and characterizing genes affecting multiple signaling pathways, e.g. *Notch* and *wg* [35]. To assess the potential role of *dPsn* in wing development, we ectopically overexpressed or RNAi silenced *dPsn* in wing disc using two wing-specific GAL4 drivers, *Sd-GAL4* and *Ptc-GAL4*.

Sd-GAL4 drives the overexpression of *dPsn* in wing disc in the pattern of *scalloped (sd)* gene, which regulates the expression of a number of targeted genes including *wg*, the central component of Wnt signaling transduction pathway [28]. Flies in which *dPsn* was silenced by RNAi in the wing by the *Sd-GAL4* driver were embryonically lethal. Compared with control flies (Sd-GAL4/+) Fig. (6A), overexpression of *dPsn* (UAS-dPsn; Sd-GAL4) in wing disc resulted in the complete loss of both wings, which were consistently observed in over 200 flies in repeated experiments Fig. (6D). We next examined the expression of wg protein by immunostaining 30 wing discs dissected from the third instar larvae with anti-wg antibody. wg was expressed as a broad strip in the notum, a thinner strip in the prospective wing margin-dorsal/ventral (D/V) boundary, and a strip encircling the prospective wing blade in WT Fig. (6B). Consistent with the phenotype observed in adult flies, there was moderately decreased wg expression in flies overexpressing *dPsn*, especially in the prospective wing blade region Fig. (6E), along with morphological alterations in wing discs. Compared with control flies Fig. (6C), wing discs of flies overexpressing *dPsn* were thinner, and reduced in size, especially in the dorsal/ventral compartment suggesting disc degeneration Fig. (6F). Together, these data showed that overexpression of *dPsn* in wing disc by *Sd-GAL4* results in severe wing malformation and reduces wg expression.

Patched (*Ptc*) is a segment polarity gene that regulates the development of wing compartments centering at the anterior/posterior border (defined between L3 and L4 vein) [29]. Compared with control flies Fig. (6G), overexpression of *dPsn* driven by *Ptc-GAL4* resulted in severe loss of intervein cells narrowing the intervein sector between L3 and L4 vein and forming extra vein cells to fill the intervein region. The intervein sector between L4 and L5 was enlarged; and pcv vein was extended Fig. (6H); in contrast, silencing of *dPsn* driven by *Ptc-GAL4* led to loss of acv vein with normal intervein cells between L3 and L4 vein Fig. (6I). Collectively, these data show that overexpression or silencing of *dPsn* in wing disc by *Ptc-GAL4* alters wing vein formation.

DISCUSSION

We have found that either overexpression or RNAi silencing of *dPsn* in *Drosophila* leads to significant changes in HR and to an irregular heartbeat rhythm accompanied with

cardiomyofibril defects. While either overexpression or silencing of *dPsn* decreased end-systolic and end-diastolic heart chamber size and increased FS compared to age-matched controls, flies in which *dPsn* was silenced exhibited an age-dependent remarkably increase in EDD and FS. Taken together, these data indicate that overexpression or RNAi silencing of *dPsn* in heart primarily leads to irregular heartbeat rhythm via regulating the electrical activity that stimulates the myocardium of the heart for contraction.

Initiation of cardiac muscle contraction requires an increase in intracellular calcium from resting concentration. The increase in intracellular calcium then triggers further release of calcium from SR stores via the Ca^{2+} release channel receptor RyR. The release of calcium can be further enhanced by activation of the Ca^{2+} release channel receptor IP_3R. This "calcium-induced calcium release" process ensures rapid and significant increases in intracellular calcium, which are essential to contraction [34]. SERCA2a transfers Ca^{2+} from the cytosol of the cell to the lumen of the SR during cardiac muscle relaxation [34]. In cultured fibroblasts from DCM patients with *PSEN1-D333G* or *PSEN2-S130L* mutations, histamine-induced resting intracellular Ca^{2+} concentrations are elevated [4]. In mouse heart muscle, Ps1 and Ps2 physically interact and colocalize with both IP_3R and the cardiac form of RyR (RyR2) to SR [36, 37]. In Ps1- and Ps2-deficient mouse embryonic fibroblasts, free Ca^{2+} concentrations in SR are decreased and IP_3R levels are increased [38]. In neuronal cells, overexpression of AD-associated *PSEN1-M146V* or *PSEN2-N141I* mutants directly increases IP_3R activity [37]. Primary hippocampal neurons from Ps1 mutant knock-in mice exhibit greatly increased levels of RyR and enhanced Ca^{2+} release [36]. Sorcin reduces the open probability of RyR2 [39]. PS2, sorcin, and RyR2 interact with each other in mouse heart [36]. Ps2- deficient mice develop normally with no evidence of cardiac hypertrophy and fibrosis, but exhibit increased cardiac contractility and potentiated peak Ca^{2+} [36]. Elevated Ca^{2+} attenuates the association of RyR2 with Ps2, and enhances the association of sorcin with Ps2 [36]. Moreover, PS1 and SERCA2a physically interact and are co-immunoprecipitated in the myocardium of DCM patients [5]. SERCA activity is diminished in fibroblasts null for both Ps1 and Ps2. Enhancing presenilin levels in Xenopus laevis oocytes accelerates clearance of cytosolic Ca^{2+} by increasing SERCA activity [40]. This suggests that the presenilins play an important role in cardiac excitation-contraction coupling and Ca^{2+} signaling via the interaction between PS2, RyR2 and sorcin, and regulation of the SERCA pump. Consistent with previous findings, we found that silencing of *dPsn* in flies elevated *dIP_3R* expression, and that overexprerssion of *dPsn* led to reduced *dRyR* expression. Silencing of *dPsn* remarkably reduced *dSERCA* expression, which together with degenerated myofibrils may lead to insufficient cardiac muscle relaxation to reduce the end-systolic and end-diastolic cardiac chamber size. These data thus provide evidence that presenilins may regulate SR Ca^{2+} storage or intracellular Ca^{2+} homeostasis in cardiac cells.

We found that 30-day old flies exhibited significantly decreased HR, increased heart chamber size and arrhythmia prevalence compared to 7-day old flies. This is consistent with previous findings indicating a decline in cardiac function with increasing age in human or *Drosophila* [41]. Compared with flies overexpressing *dPsn* or control flies, flies in which *dPsn* was silenced exhibited a more remarkably age-dependent decrease in HR and increase in EDD and arrhythmia. This indicates that silencing of *dPsn* more severely exacerbates age-dependent cardiac dysfunction than does overexpression of *dPsn* or control flies. Evidence has shown that the insulin receptor (IR) and associated pathways have a dramatic and heart-autonomous influence on age-related cardiac performance in flies, suggestive of potentially similar mechanisms in regulating cardiac aging in vertebrates [41]. IR belongs to tyrosine kinase receptor family whose activation is essential for insulin signaling in target tissues. IR undergoes PS/γ-secretase-dependent processing to produce IR intracellular domain (ICD). PS/γ-secretase inactivation resulted in reduced levels of tyrosine

autophosphorylation of the IR β-subunit upon insulin stimulation [42]. Moreover, insulin-like growth factor I receptor (IGF-IR), which shares strong structural homology with IR, was reported to be a substrate for PS/γ-secretase activity [43]. These data suggest that the PS/γ-secretase proteolysis of IR may act as a modulator of the insulin signaling pathway.

The heart forms very early during mammalian and avian embryogenesis and arises from paired mesodermal regions in the embryo. The regulation of Wnt signal transduction has been implicated as an important event that initiates cardiac development in *Drosophila* [44]. Wnts are a family of secreted signaling proteins including wg. Presenilin has been implicated in regulating Wnt signaling. First, presenilin-mediated γ-secretase activity is required for the intramembranous cleavage of Notch receptor to release notch intracellular domain (NICD) for the entry to nucleus where it induces the expression of Notch targeted genes [45]. Loss-of-function *dPsn* mutants exhibit early embryo lethality and phenotypes indicative of a general impairment of Notch signaling throughout the development in *Drosophila* [24]. This is particularly interesting in view of the fact that there is inhibitory crosstalk between the Notch and the Wnt signaling pathways (when NICD binds to Wnt) [46]. Second, PS1 negatively regulates Wnt signaling by interacting with β-catenin to facilitate β-catenin turnover *in vitro* [47–49]. β-catenin signaling is required for normal cardiac growth and development [50]. Moreover, the *PSEN1-E318G* and *PSEN1-D333G* mutations found in DCM patients [4, 5], are positioned in a large cytoplasmic loop between transmembrane domains six and seven, with which PS1 binds β-catenin [51].

We showed that overexpression of *dPsn* by *Sd-GAL4* in wing disc results in severe malformation in wing development accompanied by reduced expression of wg. These data further support the contention that presenilin negatively regulates Wnt signaling. The Notch signaling pathway plays important roles in the patterning and differentiation of the wing veins [35]. Overexpression of *dPsn* by *Ptc-GAL4* led to severe loss of intervein cells and formation of extra vein; in contrast, silencing of *dPsn* resulted in normal intervein cells but loss of acv vein. Given the known role of presenilins in γ-secretase complex [1], overexpression of *dPsn* may elevate γ-secretase activity resulting in enhanced NICD release, thereby potentiating Notch signaling to inhibit intervein cell development but promote vein cell. Conversely, silencing of *dPsn* may cause wing vein loss due to reduced γ-secretase activity. Mutations in presenilins alter the proteolytic processing of amyloid precursor protein by aberrant γ-secretase activities that results in increased neurotoxic Aβ42 production [8]. However, neither DCM-associated *PSEN2-R62H* nor *PSEN2-S130L* mutation engender significant effects on Aβ42 levels or the Aβ42/40 ratio *in vitro* [52]. In addition, treating WT mice with γ–secretase inhibitor DAPT did not alter cardiac function, including HR, left ventricle systolic and diastolic pressure [36]. These data suggest that the presenilins may regulate cardiac function through other mechanisms in addition to their effect on γ-secretase activity. Based on the previous and current findings, we propose that mutations in *PSEN1* and *PSEN2* may alter Wnt signaling via β-catenin interaction and NICD inhibitory crosstalk to ultimately cause defects in cardiac function leading to DCM pathogenesis.

In summary, we have demonstrated that either the loss or gain of *dPsn* levels in heart, results in cardiac dysfunction, owing to aberrant calcium channel receptor activities and disrupted Wnt signaling transduction. Together, these data provide novel *in vivo* evidence for pathological role(s) of the presenilins in DCM pathogenesis.

Acknowledgments

We wish to thank Mark E. Fortini for kindly providing *Drosophila* stocks and helpful suggestion, and Brett E. Bouma, Michael A. Choma, Gary Tearney, and Steven N. Fry for their helpful advice and technical assistance. This work was supported by the Cure Alzheimer's Fund [to R.E.T], National Institute of Health [R01AG014713 and

R01MH60009 to R.E.T; R01CA75289 and R01HL095717 to J.G.F], Air Force Office of Scientific Research [FA9550-07-1-0014 to J.G.F], and the Neuroscience Education and Research Foundation [to A.L.]. The Microscopy Core Facility at the MGH Program in Membrane Biology receives support from the Boston Area Diabetes and Endocrinology Research Center [DK 57521] and the Center for the Study of Inflammatory Bowel Disease [DK 43351].

References

1. De Strooper B. Aph-1, Pen-2, and Nicastrin with Presenilin generate an active gamma-Secretase complex. Neuron. 2003; 38:9–12. [PubMed: 12691659]
2. De Strooper B. Loss-of-function presenilin mutations in Alzheimer disease. Talking Point on the role of presenilin mutations in Alzheimer disease. EMBO Rep. 2007; 8:141–146. [PubMed: 17268505]
3. Selkoe DJ. The cell biology of beta-amyloid precursor protein and presenilin in Alzheimer's disease. Trends Cell Biol. 1998; 8:447–453. [PubMed: 9854312]
4. Li D, Parks SB, Kushner JD, Nauman D, Burgess D, Ludwigsen S, et al. Mutations of presenilin genes in dilated cardiomyopathy and heart failure. Am J Hum Genet. 2006; 79:1030–1039. [PubMed: 17186461]
5. Gianni D, Li A, Tesco G, McKay KM, Moore J, Raygor K, et al. Protein aggregates and novel presenilin gene variants in idiopathic dilated cardiomyopathy. Circulation. 2010; 121:1216–1226. [PubMed: 20194882]
6. Grogan M, Redfield MM, Bailey KR, Reeder GS, Gersh BJ, Edwards WD, et al. Long-term outcome of patients with biopsy-proved myocarditis: comparison with idiopathic dilated cardiomyopathy. J Am Coll Cardiol. 1995; 26:80–84. [PubMed: 7797779]
7. To MD, Gokgoz N, Doyle TG, Donoviel DB, Knight JA, Hyslop PS, et al. Functional characterization of novel presenilin-2 variants identified in human breast cancers. Oncogene. 2006; 25:3557–3564. [PubMed: 16474849]
8. Scheuner D, Eckman C, Jensen M, Song X, Citron M, Suzuki N, et al. Secreted amyloid beta-protein similar to that in the senile plaques of Alzheimer's disease is increased *in vivo* by the presenilin 1 and 2 and APP mutations linked to familial Alzheimer's disease. Nat Med. 1996; 2:864–870. [PubMed: 8705854]
9. Sanbe A, Osinska H, Villa C, Gulick J, Klevitsky R, Glabe CG, et al. Reversal of amyloid-induced heart disease in desmin-related cardiomyopathy. Proc Natl Acad Sci USA. 2005; 102:13592–13597. [PubMed: 16155124]
10. Strittmatter WJ, Saunders AM, Schmechel D, Pericak-Vance M, Enghild J, Salvesen GS, et al. Apolipoprotein E: high-avidity binding to beta-amyloid and increased frequency of type 4 allele in late-onset familial Alzheimer disease. Proc Natl Acad Sci USA. 1993; 90:1977–1981. [PubMed: 8446617]
11. Bennet AM, Di Angelantonio E, Ye Z, Wensley F, Dahlin A, Ahlbom A, et al. Association of apolipoprotein E genotypes with lipid levels and coronary risk. JAMA. 2007; 298:1300–1311. [PubMed: 17878422]
12. Chow N, Bell RD, Deane R, Streb JW, Chen J, Brooks A, et al. Serum response factor and myocardin mediate arterial hypercontractility and cerebral blood flow dysregulation in Alzheimer's phenotype. Proc Natl Acad Sci USA. 2007; 104:823–828. [PubMed: 17215356]
13. Wu Z, Guo H, Chow N, Sallstrom J, Bell RD, Deane R, et al. Role of the MEOX2 homeobox gene in neurovascular dysfunction in Alzheimer disease. Nat Med. 2005; 11:959–965. [PubMed: 16116430]
14. Donoviel DB, Hadjantonakis AK, Ikeda M, Zheng H, Hyslop PS, Bernstein A. Mice lacking both presenilin genes exhibit early embryonic patterning defects. Genes Dev. 1999; 13:2801–2810. [PubMed: 10557208]
15. Nakajima M, Moriizumi E, Koseki H, Shirasawa T. Presenilin 1 is essential for cardiac morphogenesis. Dev Dyn. 2004; 230:795–799. [PubMed: 15254914]
16. Ocorr K, Reeves NL, Wessells RJ, Fink M, Chen HS, Akasaka T, et al. KCNQ potassium channel mutations cause cardiac arrhythmias in Drosophila that mimic the effects of aging. Proc Natl Acad Sci USA. 2007; 104:3943–3948. [PubMed: 17360457]

17. Vigoreaux JO. Genetics of the Drosophila flight muscle myofibril: a window into the biology of complex systems. Bioessays. 2001; 23:1047–1063. [PubMed: 11746221]
18. Paternostro G, Vignola C, Bartsch DU, Omens JH, McCulloch AD, Reed JC. Age-associated cardiac dysfunction in Drosophila melanogaster. Circ Res. 2001; 88:1053–1058. [PubMed: 11375275]
19. Curtis NJ, Ringo JM, Dowse HB. Morphology of the pupal heart, adult heart, and associated tissues in the fruit fly, Drosophila melanogaster. J Morphol. 1999; 240:225–235. [PubMed: 10367397]
20. Huang D, Swanson EA, Lin CP, Schuman JS, Stinson WG, Chang W, et al. Optical Coherence Tomography. Science. 1991; 254:1178–1181. [PubMed: 1957169]
21. Drexler W, Morgner U, Ghanta RK, Kärtner FX, Schuman JS, Fujimoto JG. Ultrahigh-resolution ophthalmic optical coherence tomography. Nat Med. 2001; 7:502–507. [PubMed: 11283681]
22. Tearney GJ, Brezinski ME, Bouma BE, Boppart SA, Pitvis C, Southern JF, et al. *In vivo* endoscopic optical biopsy with optical coherence tomography. Science. 1997; 276:2037–2039. [PubMed: 9197265]
23. Wolf MJ, Amrein H, Izatt JA, Choma MA, Reedy MC, Rockman HA. Drosophila as a model for the identification of genes causing adult human heart disease. Proc Natl Acad Sci USA. 2006; 103:1394–1399. [PubMed: 16432241]
24. Guo Y, Livne-Bar I, Zhou L, Boulianne GL. Drosophila presenilin is required for neuronal differentiation and affects notch subcellular localization and signaling. J Neurosci. 1999; 19:8435–8442. [PubMed: 10493744]
25. Ye Y, Fortini ME. Apoptotic activities of wild-type and Alzheimer's disease-related mutant presenilins in Drosophila melanogaster. J Cell Biol. 1999; 146:1351–1364. [PubMed: 10491396]
26. Hay BA, Wolff T, Rubin GM. Expression of baculovirus P35 prevents cell death in Drosophila. Development. 1994; 120:2121–2129. [PubMed: 7925015]
27. Kramer JM, Staveley BE. GAL4 causes developmental defects and apoptosis when expressed in the developing eye of Drosophila melanogaster. Genet Mol Res. 2003; 2:43–47. [PubMed: 12917801]
28. Paumard-Rigal S, Zider A, Vaudin P, Silber J. Specific interactions between vestigial and scalloped are required to promote wing tissue proliferation in Drosophila melanogaster. Dev Genes Evol. 1998; 208:440–446. [PubMed: 9799424]
29. Speicher SA, Thomas U, Hinz U, Knust E. The Serrate locus of Drosophila and its role in morphogenesis of the wing imaginal discs: control of cell proliferation. Development. 1994; 120:535–544. [PubMed: 8162853]
30. Brand AH, Perrimon N. Targeted gene expression as a means of altering cell fates and generating dominant phenotypes. Development. 1993; 118:401–415. [PubMed: 8223268]
31. Park, A. Psn constructs and insertions. FlyBase; 2004. (www.flybase.org)
32. Sullivan William, MA. R Scott Hawley. Drosophila Protocols. Vol. 245. Cold Spring Harbor Labroratory Press; 2000.
33. Zikova M, Da Ponte JP, Dastugue B, Jagla K. Patterning of the cardiac outflow region in Drosophila. Proc Natl Acad Sci USA. 2003; 100:12189–12194. [PubMed: 14519845]
34. Berridge MJ, Lipp P, Bootman MD. The versatility and universality of calcium signalling. Nat Rev Mol Cell Biol. 2000; 1:11–21. [PubMed: 11413485]
35. Sturtevant MA, Bier E. Analysis of the genetic hierarchy guiding wing vein development in Drosophila. Development. 1995; 121:785–801. [PubMed: 7720583]
36. Takeda T, Asahi M, Yamaguchi O, Hikoso S, Nakayama H, Kusakari Y, et al. Presenilin 2 regulates the systolic function of heart by modulating Ca^{2+} signaling. FASEB J. 2005; 19:2069–2071. [PubMed: 16204356]
37. Cheung KH, Shineman D, Muller M, Cardenas C, Mei L, Yang J, et al. Mechanism of Ca^{2+} disruption in Alzheimer's disease by presenilin regulation of InsP3 receptor channel gating. Neuron. 2008; 58:871–883. [PubMed: 18579078]
38. Kasri NN, Kocks SL, Verbert L, Hebert SS, Callewaert G, Parys JB, et al. Up-regulation of inositol 1,4,5-trisphosphate receptor type 1 is responsible for a decreased endoplasmic-reticulum Ca2+ content in presenilin double knock-out cells. Cell Calcium. 2006; 40:41–51. [PubMed: 16675011]

39. Lokuta AJ, Meyers MB, Sander PR, Fishman GI, Valdivia HH. Modulation of cardiac ryanodine receptors by sorcin. J Biol Chem. 1997; 272:25333–25338. [PubMed: 9312152]
40. Green KN, Demuro A, Akbari Y, Hitt BD, Smith IF, Parker I, et al. SERCA pump activity is physiologically regulated by presenilin and regulates amyloid beta production. J Cell Biol. 2008; 181:1107–1116. [PubMed: 18591429]
41. Ocorr K, Akasaka T, Bodmer R. Age-related cardiac disease model of Drosophila. Mech Ageing Dev. 2007; 128:112–116. [PubMed: 17125816]
42. Kasuga K, Kaneko H, Nishizawa M, Onodera O, Ikeuchi T. Generation of intracellular domain of insulin receptor tyrosine kinase by gamma-secretase. Biochem Biophys Res Commun. 2007; 360:90–96. [PubMed: 17577576]
43. McElroy B, Powell JC, McCarthy JV. The insulin-like growth factor 1 (IGF-1) receptor is a substrate for gamma-secretase-mediated intramembrane proteolysis. Biochem Biophys Res Commun. 2007; 358:1136–1141. [PubMed: 17524361]
44. Eisenberg LM, Eisenberg CA. Wnt signal transduction and the formation of the myocardium. Dev Biol. 2006; 293:305–315. [PubMed: 16563368]
45. Selkoe D, Kopan R. Notch and Presenilin: regulated intramembrane proteolysis links development and degeneration. Annu Rev Neurosci. 2003b; 26:565–597. [PubMed: 12730322]
46. Wesley CS. Notch and wingless regulate expression of cuticle patterning genes. Mol Cell Biol. 1999; 19:5743–5758. [PubMed: 10409762]
47. Zhang Z, Hartmann H, Do VM, Abramowski D, Sturchler-Pierrat C, Staufenbiel M, et al. Destabilization of beta-catenin by mutations in presenilin-1 potentiates neuronal apoptosis. Nature. 1998; 395:698–702. [PubMed: 9790190]
48. Nishimura M, Yu G, Levesque G, Zhang DM, Ruel L, Chen F, et al. Presenilin mutations associated with Alzheimer disease cause defective intracellular trafficking of beta-catenin, a component of the presenilin protein complex. Nat Med. 1999; 5:164–169. [PubMed: 9930863]
49. Soriano S, Kang DE, Fu M, Pestell R, Chevallier N, Zheng H, et al. Presenilin 1 negatively regulates beta-catenin/T cell factor/lymphoid enhancer factor-1 signaling independently of beta-amyloid precursor protein and notch processing. J Cell Biol. 2001; 152:785–794. [PubMed: 11266469]
50. Liebner S, Cattelino A, Gallini R, Rudini N, Iurlaro M, Piccolo S, et al. Beta-catenin is required for endothelial-mesenchymal transformation during heart cushion development in the mouse. J Cell Biol. 2004; 166:359–367. [PubMed: 15289495]
51. Murayama M, Tanaka S, Palacino J, Murayama O, Honda T, Sun X, et al. Direct association of presenilin-1 with beta-catenin. FEBS Lett. 1998; 433:73–77. [PubMed: 9738936]
52. Walker ES, Martinez M, Brunkan AL, Goate A. Presenilin 2 familial Alzheimer's disease mutations result in partial loss of function and dramatic changes in Abeta 42/40 ratios. J Neurochem. 2005; 92:294–301. [PubMed: 15663477]

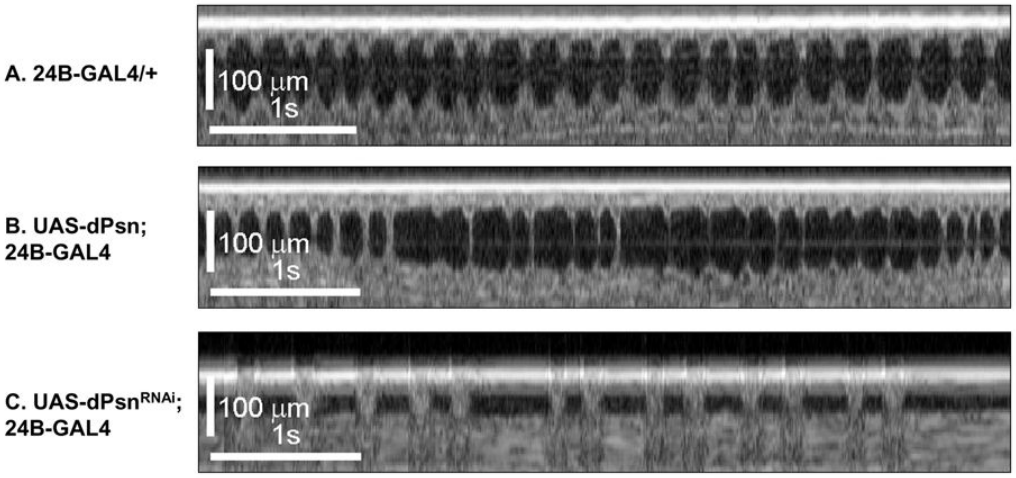

Fig. 1.

Representative M-mode optical coherence tomography (OCT) imaging of cardiac function in 30-day old adult *Drosophila*. A: Control showed normal heart rate (HR): 250 beat per minute (BPM) and rhythm; B. Overexpression of *dPsn* led to increased HR (296BPM) and irregular heartbeats; C: Silencing of *dPsn* caused reduced HR (167BPM), small heart chamber and irregular heartbeat.

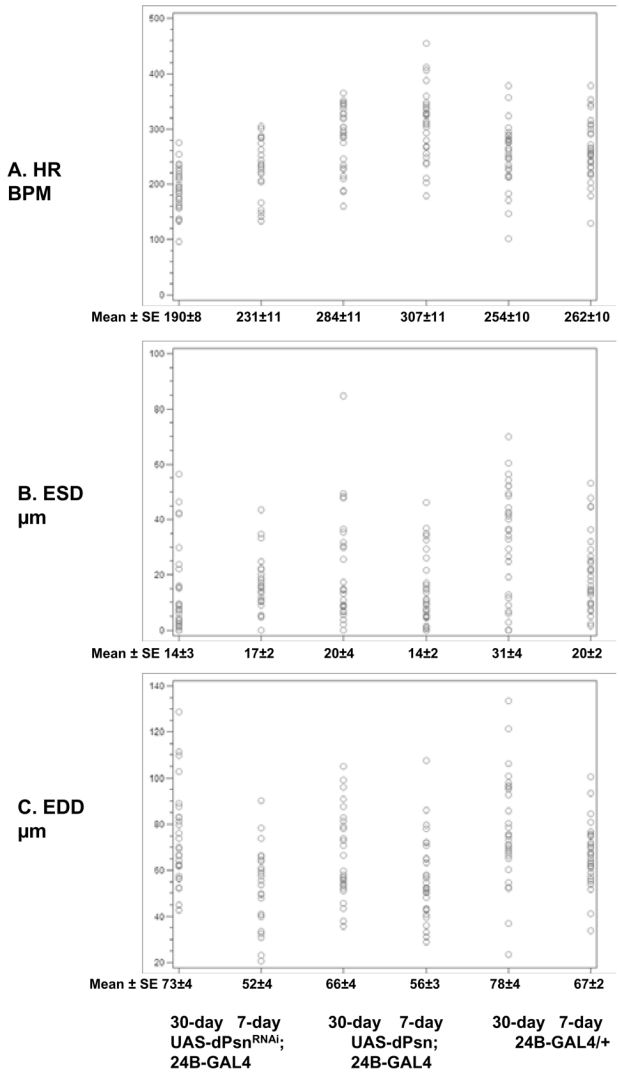

Fig. 2.

Scatter plots of heart rate (HR), end-systolic vertical dimension (ESD) and end-diastolic vertical dimension (EDD), respectively, of flies in each tested group, generated using a SAS GLM program. A. HR (beat per minute, BPM); B: ESD (μm); C: EDD (μm). Mean ± SE for each tested group is shown.

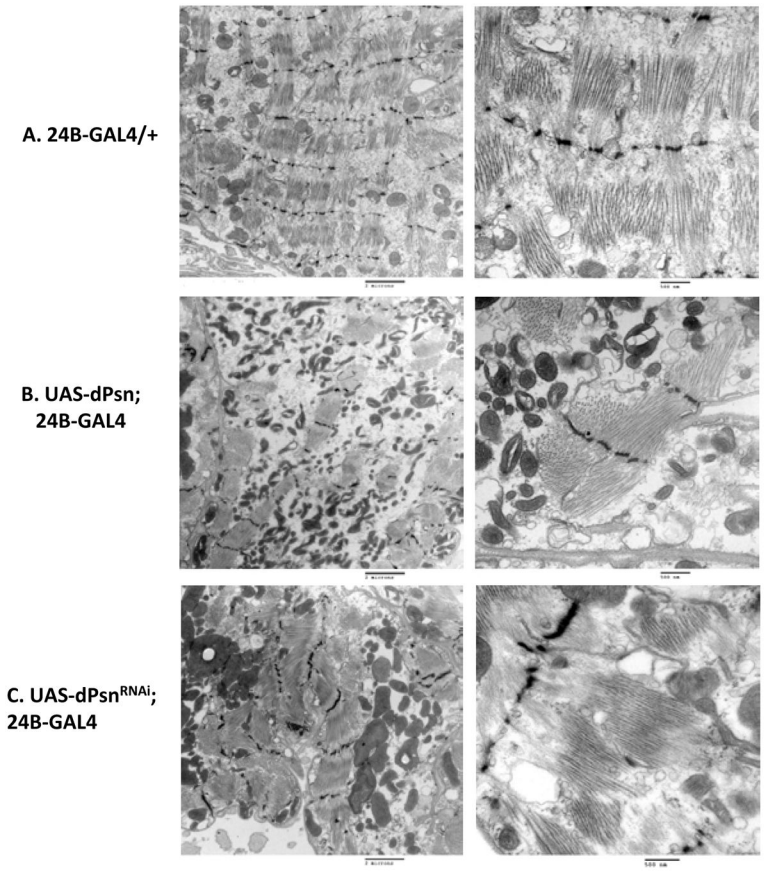

Fig. 3.

Transmission electron microscopy of the myofibril. A: Controls showed normal myofibril structure; B: Overexpression of *dPsn* led to loss of regular structure with vacuoles, a broadening of Z-line and swollen mitochondria in myofibril; C: Silencing of *dPsn* caused an overall decrease in the density of myofibrils with vacuoles, a breaking Z-line, and severely degenerative mitochondria with impaired structure in myofibril. *Magnification*: Left: 10,000X, *Scale bar*: 2μm. Right: 30,000X, *Scale bar*: 500nm.

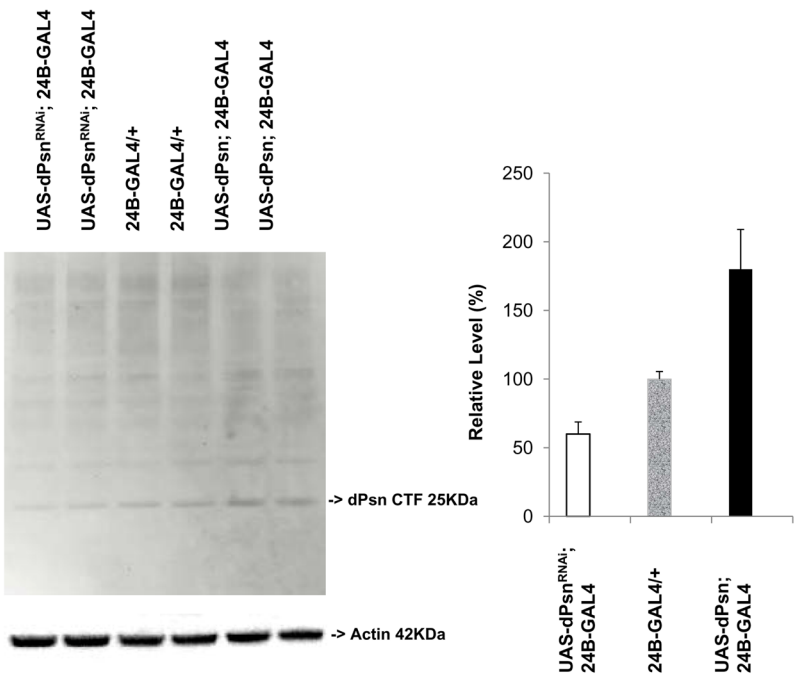

Fig. 4.

Western Blotting by anti-dPsn detected *dPsn* –C-terminal fragment (CTF) (25 KDa) in the heart and muscle of controls and transgenic flies in which *dPsn* was silenced or overexpressed. The dPsn expression level was normalized with respect to dActin (42KDa) loading control. Silencing of *dPsn* led to a 60% decrease in dPsn expression, and overexpression of *dPsn* led to a 180% increase in dPsn expression as compared to controls.

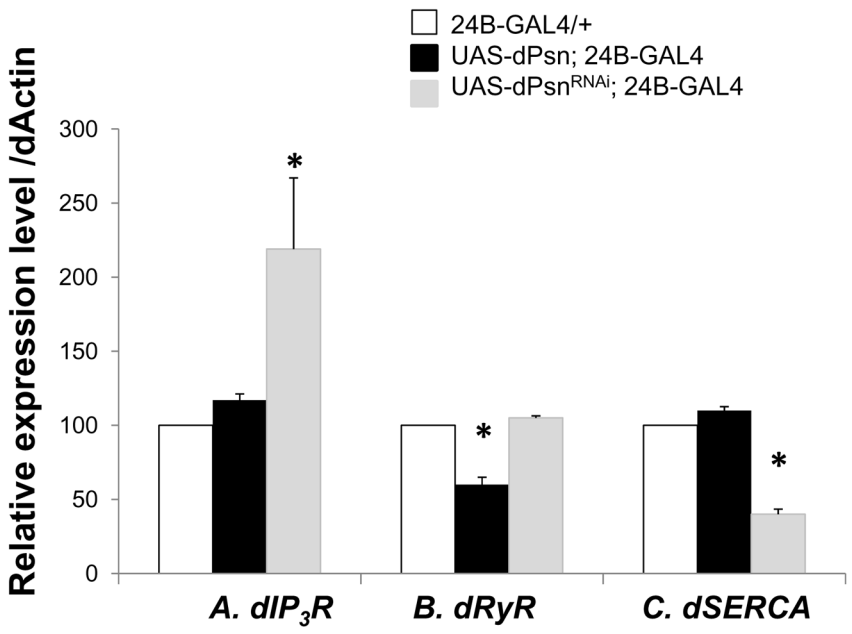

mRNA%	A. *dIP$_3$R*	B. *dRyR*	C. *dSERCA*
24B-GAL4	100	100	100
UAS-dPsn; 24B-GAL4	117± 4.2	60± 5* (p=0.04)	110 ±2.6
UAS-dPsn^{RNAi}; 24B-GAL4	219 ±48* (p=0.01)	105± 1.4	40± 3.5* (p=0.02)

Fig. 5.

Quantification of relative *Drosophila* inositol 1,4,5-trisphosphate receptor (*dIP$_3$R*), the ryanodine receptor (*dRyR*) and the SR Ca^{2+}-ATPase pump SERCA2a (*dSERCA*) expression by real-time PCR using SYBR Green. A: *dIP3R*: overexpression of *dPsn* increased *dIP3R* level 1.17-fold; silencing of *dPsn* increased *dIP3R* expression 2.19-fold. B: *dRyR*: overexpression of *dPsn* decreased *dRyR* expression to 60%; silencing of *dPsn* increased *dRyR* expression 1.05-fold. C: *dSERCA:* overexpression of *dPsn* increased *dSERCA* level 1.1-fold; silencing of *dPsn* decreased *dSERCA* expression to 40%. Results are shown as Mean ± Std of repeated experiments. *Asterisks* (*) denote results with $p<0.05$ compared to control levels.

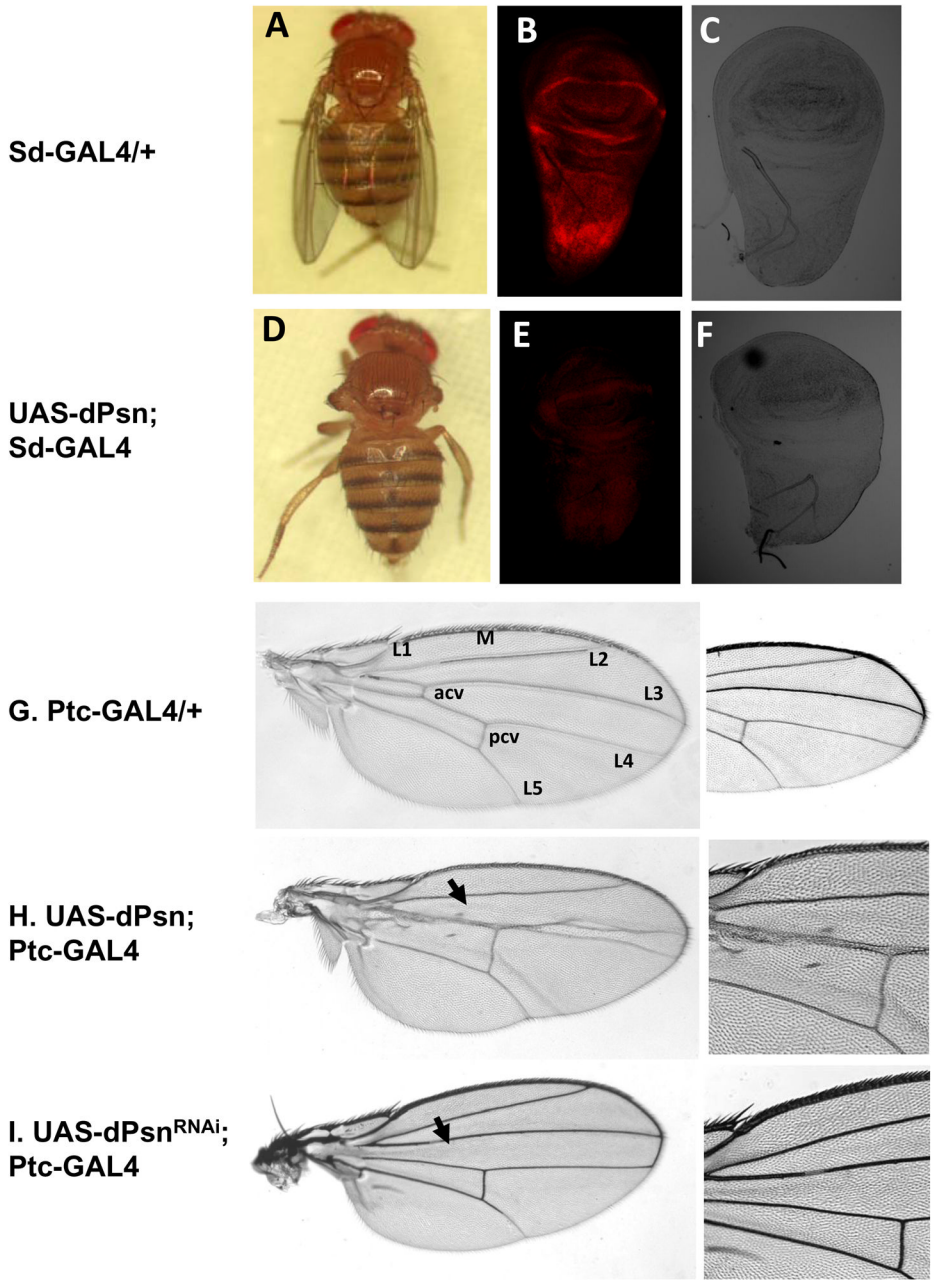

Fig. 6.

Overexpression or silencing of *dPsn* in the wing. A. B. C. Control flies had normal wings (**A**), and wg expression (**B**) on normal wing disc (**C**). D. E. F. Overexpression of *dPsn* in the wing disc by *Sd-GAL4* led to complete loss of both wings (**D**) and moderately decreased wg expression (**E**) on a thinner and smaller wing disc (**F**). G. Control fly wings have five longitudinal (L1-5) and two cross-veins: anterior (acv) and posterior (pcv), creating distinct intervein sectors. **H.** Overexpression of *dPsn* in the wing by *Ptc-GAL4* led to loss of intervein cells between L3 and L4 vein. The intervein sector between L4 and L5 was enlarged and pcv vein was extended. **I.** silencing of *dPsn* in the wing by *Ptc-GAL4* led to loss of acv vein in the intervein sector between L3 and L4 vein.

Table 1

Cardiac Functions of Adult Flies

Parameter		HR (BPM) (Mean ± SE)	ESD (μm) (Mean ± SE)	EDD (μm) (Mean ± SE)	FS (%)(Mean ± SE)	Arrhythmia Prevalence (%)
7D	24B-GAL4/+ (Control) N=31	262 ± 10	20 ± 2	67 ± 2	69 ± 4	8 (26%)
	UAS-dPsn; 24B-GAL4 N=31	307 ± 11 *** (p=0.001) ↑	14 ± 2	56 ± 3 * (p=0.03) ↓	76 ± 3	6 (19%)
	UAS-dPsn^{RNAi}; 24B-GAL4 N=24	231 ± 11 *(p=0.04) ↓	17 ± 2	52 ± 4 ** (p=0.006) ↓	67 ± 4	11 (46%)
	Total N=86	269 ± 7	17 ± 1	58 ± 2	71 ± 2	25 (29%)
30D	24B-GAL4/+ (Control) N=30	254 ± 10	31 ± 4 # (p=0.008) ↑	78 ± 4 # (p=0.02) ↑	62 ± 4	8 (27%)
	UAS-dPsn; 24B-GAL4 N=28	284 ± 11 * (p=0.04) ↑	20 ± 4 * (p=0.01) ↓	66 ± 4 *(p=0.02) ↓ # (p=0.04) ↑	69 ± 5	13 (46%) # (p=0.03) ↑
	UAS-dPsn^{RNAi}; 24B-GAL4 N=28	190 ± 8 **** (p<0.0001) ↓ ## (p=0.008) ↓	14 ± 3 ****(p<0.0001) ↓	73 ± 4 #### (p<0.0001) ↑	83 ± 4 ***(p=0.0002) ↑ ## (p=0.005) ↑	16 (57%) ** (p=0.01) ↑
	Total N=86	243 ± 7 ## (p=0.005) ↓	22 ± 2 # (p=0.04) ↑	73 ± 2 #### (p<0.0001) ↑	71 ± 2	37 (43%)
7D and 30D	24B-GAL4/+ (Control) N=61	258 ± 7	26 ± 2	72 ± 3	66 ± 3	16 (26%)
	UAS-dPsn; 24B-GAL4 N=59	296 ± 8 *** (p=0.0002) ↑	17 ± 2 ** (p=0.004) ↓	61 ± 2 ***(p=0.001) ↓	73 ± 3	19 (32%)
	UAS-dPsn^{RNAi}; 24B-GAL4 N=52	209 ± 7 **** (p<0.0001) ↓	15 ± 2 *** (p=0.0004) ↓	63 ± 3 **(p=0.009) ↓	75 ± 3 * (p=0.02) ↑	27 (54%) ** (p=0.01) ↑

HR: Heart rate.

EDD: End-diastolic dimension. ESD: End-systolic dimension. FS: Fractional shortening.

* p<0.05,

** p<0.01,

*** p<0.001,

**** p<0.0001: vs. Age-matched controls;

# $p<0.05$,

$p<0.01$,

$p<0.001$,

$p<0.0001$: vs. 7-day old age group,

↑ shows significant increase;

↓ shows significant decrease.